The Effect of an External applied Far Field Tensile Stress on the Early Stages of Ageing in a 7475 Aerospace Alloy

The Effect of an External applied Far Field Tensile Stress on the Early Stages of Ageing in a 7475 Aerospace Alloy

D.Bakavos[1], P.B.Prangnell[1], G. Sha[2], A.Cerezo[2],
[1]School of Materials, University of Manchester, U.K.
[2]Department of Materials, University of Oxford, UK.

1 Introduction

It is now well established, in aluminium 2xxx series alloys, that the application of far field stress can alter the microstructure development during ageing [1-4] and in some cases the alloy's resultant mechanical properties [5]. Residual stresses retained after heat treatment can also influence the early stages of ageing in some alloys [6]. Research has shown that above a critical threshold stress the nucleation of thin plate shaped phases (e.g. GP zones, θ″, θ′ and Ω) with a large plate normal matrix misfit can be biased on to specific habit plane-variants, preferentially aligned with the applied stress field. This stress threshold is quite low for Cu GP zones/θ″ (~20 MPa), but higher for θ′ (~ 30 MPa) and Ω (~120 MPa) [1-4,6] and is also affected by the ageing temperature and composition [2]. As well as biasing habit plane selection, the applied stress can result in changes in precipitate size and morphology [1-4].

In contrast, very limited work has been published that investigates similar phenomena in 7xxx series alloys, especially during the early stages of aging where it is possible to produce both spherical (GP-I) and plate morphology (GP-II) GP zones, depending on the composition and aging treatment [7]. GP-II zones tend to be more stable at higher temperatures and more dominant in alloys with low Cu content [10,13]. Of particular relevance is the use of 7xxx alloys in aerospace applications where components are manufactured by creep-ageforming, which subjects plates to bending stresses that are subsequently partially relaxed during the application of an artificial ageing treatment [8]. A preliminary qualitative investigation of the behaviour of a 7475 alloy indicated little obvious effect of stress-ageing with no preferential alignment of the η′ or η precipitates being observed [3]. However, subsequent more detailed research of the whole ageing sequence, based on TEM and quantitative SAXS analysis, detected subtle differences in diffraction data that were tentatively attributed to the applied tensile stress influencing the early stages of precipitation, by promoting GP-II zones, and accelerated overageing caused by dislocation creep [7]. Here we hope to extend this work to provide corroborating evidence for the proposed influence of an applied stress on early stage ageing behaviour in 7xxx alloys, by investigating the development of GP zones in more detail, with the aid of HRTEM and 3D Atom Probe techniques (3DAP). In this work we have again studied the same 7475 alloy previously investigated [3-4,7].

2 Experimental

The 7475 alloy used in this work was supplied by Alcan as a 60 mm thick plate in a T351 condition, after solution treatment and stretching by 2%. 8 mm ϕ by 55 mm gauge length ten-

sile specimens were machined from the ¼ / ¾ plate thickness positions parallel to the rolling direction. These samples were subjected to constant stress-ageing treatments at the highest load possible without failing, of 245 MPa, for a range of times at 108 °C, through the first step of a T7351 two-stage ageing treatment, with an initial ramp rate of 75 °C/hour. It should be noted that the specimens had been naturally aged over 6 months prior to heat treatment. Stress-free control samples were aged identically by simultaneously positioning them at the same height in the furnace. An FEI Tecnai F30 FEGTEM and a Philips CM200 TEM was used to characterise the precipitate structures in the aged specimens. The loading direction for the stress-aged samples was marked on the specimen foils before polishing. The precipitates present were further characterised by 3DAP analysis using the Imago Scientific Instruments LEAP(TM) 3000X Si instrument at the Opal facility in Oxford. Needle- shaped specimens for the LEAP were prepared by the standard two-stage electropolishing method, and analysis was carried out at a specimen temperature of 27K with a pulse fraction of 20 % in ultra-high vacuum ($<10^{-10}$Torr). Small Angle X-ray Scattering (SAXS) experiments were performed at the CCLRC Daresbury Laboratory, UK, (beam line 2.1). After instrument and background corrections the SAXS data was analysed, following the method described in [9], to obtain the Guinier radius (R_g), by using an iterative procedure involving fitting the slope of integrated intensity vs. scattering vector (I vs. q) plots in the region of the $0.8R_g < q < 1.8R_g$ Kratky plot. By assuming random alignment of the precipitates, this was converted into a 'mean sphere radius' [9].

3 Results and Discussion

Careful comparison of the age-hardening curves for the stress-free and stress-aged samples (Fig. 1) showed that slight differences emerged by the end of the first ageing stage (4 hrs at 108 °C). The samples started in the T351 condition with a relatively high hardness level, resulting from extended natural ageing for 6 months, and softened with time due to some GP zone reversion occurring at the ageing temperature. However, the curves diverged slightly with the stress-aged sample developing a ~ 2 % lower hardness than the stress-free control.

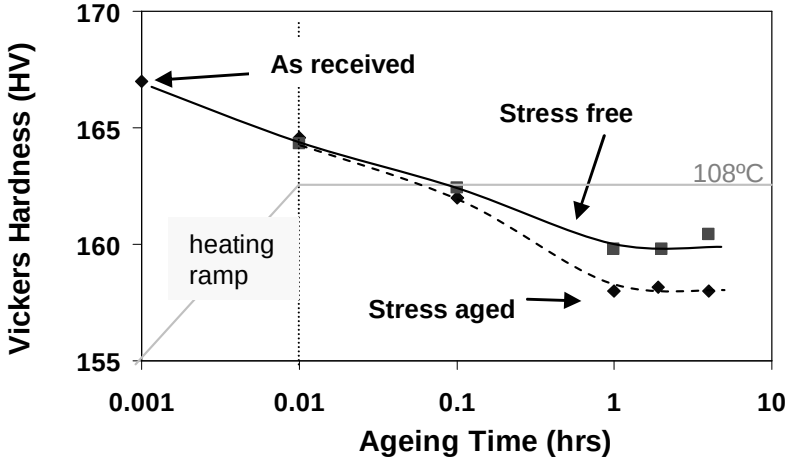

Figure 1: hardness curves for the first stage of a T73 temper (at 108 °C), comparing ageing under a constant tensile stress of 245 MPa and stress-free.

At the end of the first heating ramp $<001>_{Al}$ projection diffraction patterns from both samples contained rows of diffuse diffraction spots along $<220>_{Al}$ directions characteristic of internally ordered spherical morphology GP-I zones with a $\{001\}_{Al}$ habit plane [10,14]. In addition, careful examination of the $[111]_{Al}$ projections, shown in Fig. 2, reveled an extra set of

elongated pairs of reflections, only seen with the stress-aged sample, slightly outside the {422}/3 position. Similar reflections have been attributed to the presence of GP-II zones in ternary Al-Zn-Mg alloys, which have a plate morphology and a $\{111\}_{Al}$ habit plane [10-15]. The origin of the weaker spot within the pairs of reflections is probably the result of double diffraction, via a 220-type matrix reflection [10].

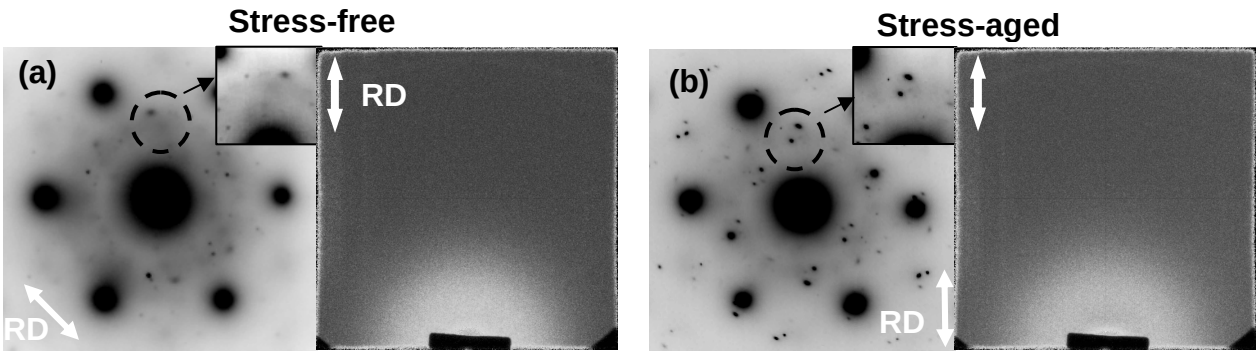

Figure 2: Comparison of TEM $<111>_{Al}$ SAED (with enlarged inserts) and SAXS diffraction patterns for; (a) the stress-free aged condition and (b) stress-aged 7475 samples immediately after the heating ramp at the beginning of the first 108 °C temper stage.

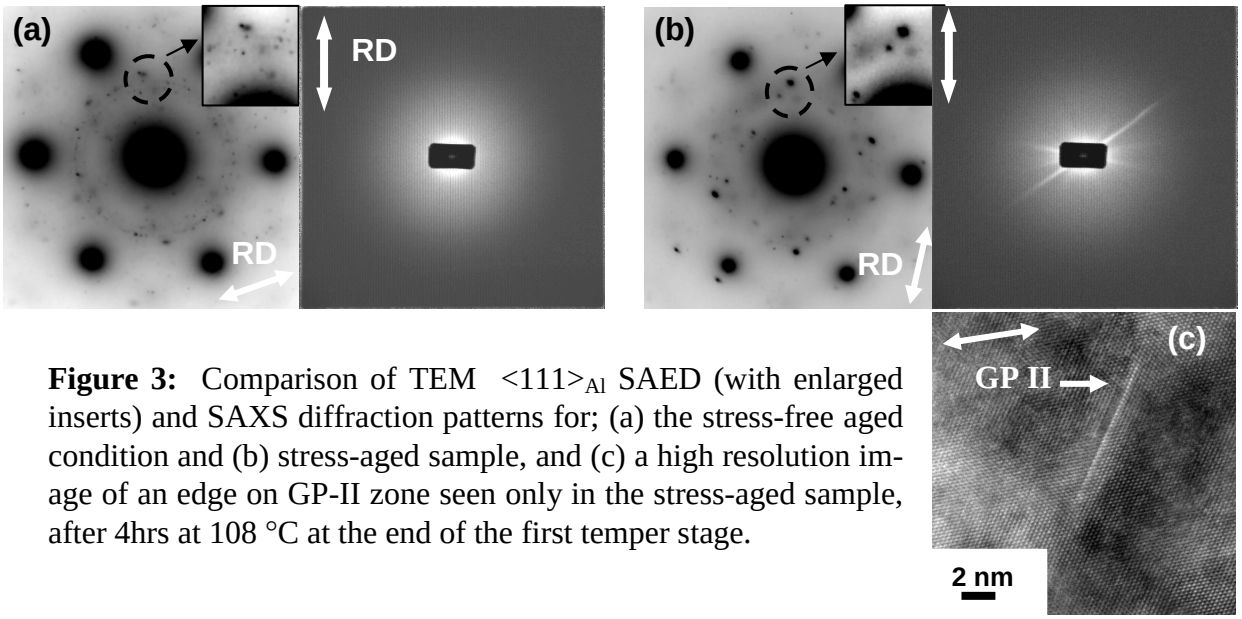

Figure 3: Comparison of TEM $<111>_{Al}$ SAED (with enlarged inserts) and SAXS diffraction patterns for; (a) the stress-free aged condition and (b) stress-aged sample, and (c) a high resolution image of an edge on GP-II zone seen only in the stress-aged sample, after 4hrs at 108 °C at the end of the first temper stage.

From analysis of the SAXS diffraction patterns at the end of the first heating ramp (Fig. 2) it was found that the average scattering intensities were isotropic. This indicates that the GP zones present at this stage are mostly approximately spherical in morphology (GP-I), or that there is no strong preferential alignment of any plate shaped zones. This is in agreement with the observations of several researchers [10,13-14], who report that predominantly low aspect ratio, or spherical, GP-I zones nucleate during natural ageing in Al-Zn-Mg-Cu alloys, and these partially revert and coarsen during the first heating ramp [13]. However, even at this stage a very small difference in the average size of the GP zones was noted for the stress-free and stress-aged conditions of R_g=14.06 Å and R_g=15.1 Å (±0.1) respectively.

After the end of the first ageing stage (4 hrs at 108 °C) comparison of the SAED diffraction spot intensities (Fig. 2b & Fig.3b) suggested that the volume fraction of the plate shaped GP-II zones had increased in the stress-aged samples, whereas the stress-free coupons still

contained mainly spherical GP-I zones (Fig.3a). Furthermore, very thin, sometimes monolayer, plate shaped GP zones were now readily identifiable by high resolution TEM - but only in the stress-aged specimens (Fig. 3c). These extremely small plate shaped precipitates are similar to those identified as GP-II zones by Berg et al. [10]. SAXS results also showed that the difference in the average precipitate size became more significant at the end of the first ageing stage, with R_g averaged over the full angular range increasing to 16.8 Å and 14.4 Å, for the conventional and stress-aged samples respectively. In addition, while the intensity distribution in the SAXS diffraction patterns for the stress-free sample remained isotropic, the constant stress-aged alloy in Fig.3 (b) showed the presence of local aligned streaks immerging from the background.

Similar SAXS diffraction intensity streaks have been observed in other alloy systems where thin {111} habit plane, plate-shaped, precipitates are present in the microstructure [12]. Here, the individual streaks must originate from preferentially aligned thin GP-II zones (as exemplified in Fig. 3c) within individual grains from the polycrystalline sample and tended to be grouped at around 50–60° to the tensile axis. This corresponds to a preferred habit plane orientation of ~ 35° to the tensile axis. At this ageing time the relative integrated intensities for the stress-aged sample were found to be significantly lower than for the stress-free condition, with a larger difference than seen at the top of the first heating ramp, suggesting, in line with the hardness measurements, that the volume fraction of the GP zones was smaller in the stress-aged alloy. Sector integrated analysis (±4°) along streaks at 55° relative to the stress axis resulted in an R_g ~14.2 Å (±0.1), compared to R_g ~10.4 Å (±0.1) from the more isotropic SAXS background intensity. Subtracting the data for the isotropic area from aligned streaks gave the thickness of the plate shaped GP-II zone of 3.8 Å (±0.1), which compares favorably to an average plate thickness measured from HRTEM images of 3.5 Å (±0.1).

3DAP reconstructed volumes showing the Zn, Mg, and Cu atom species concentrated within clusters/precipitates in the stress-free and stress-aged samples after 4 hrs at 108^{o}C are shown in Fig.4. The average statistical data obtained from such regions of high solute enrichment is summarised in table 1. The results in table 1 are discriminated into two groups based on the Zn/Mg ratio, which, for the average composition of groups of particles with a similar morphology and size range, was polarised as either close to ~ 1.3 or ~ 1.0. For the stress-free sample larger low-aspect ratio spherical/ellipsoidal GP-I zone clusters dominated the microstructure with a Zn/Mg ratio of 1.02, a (Zn+Cu)/Mg ratio of 1.17, and an average size of ~2- 4 nm. The analysed volume also contained some larger plates having a higher Zn/Mg ratio of 1.35. Other atom probe studies have reported GP zone Zn/Mg ratios in Al-Zn-Mg-Cu alloys to be in the range 1 - 1.3, but most commonly reported values are close to 1 [13-17]. In a 7050 alloy aged for 4 hrs at 140°C, which has a higher Zn and Cu level but a similar Mg concentration, Sha and Cerezo have previously found the Mg/Zn ratio of fine GP zones to be ~ 1.3 and (Zn+Cu)/Mg to be 1.4. Other workers have reported Zn/Mg ratios of close to ~1.3 for the η′ phase which contains more Cu [14-18]. In contrast to the stress-free material, in the stress-aged sample the analysed volume was dominated by smaller 1-3 nm and, on average, higher aspect ratio zones with a Zn/Mg ratio of 1.34. However, this sample also contained some larger lower aspect ratio zones with a lower average Zn/Mg ratio ~ 1.16. The average Cu content of the solute rich regions was also reduced in the stress-aged sample. Overall the volume fraction of identifiable solute rich zones was lower in the stress-aged sample, in agreement with the weaker integrated SAXS intensities and lower hardness levels, which showed that a greater degree of reversion occurred in the stress-aged sample.

Combining the above TEM, SAXS, and 3DAP evidence, it can be concluded that in the first low temperatures ageing stage, without the application of a stress, mainly GP-I zones are seen in the 7475 alloy that first develop on naturally ageing and survive reversion during the heating ramp. In comparison, with a stress applied during ageing, it is clear that less GP-I zones are retained and that they are in competition with the development of thin plate shaped GP-II zones. GP-II zones are known to normally form preferentially at higher ageing temperatures in low Cu content alloys [10-11], but have also been reported in Al-Zn-Mg-Cu alloys [13,16]. Similar to plate morphology phases and disc shaped Cu GP zones in Al-Cu alloys [1,6], GP-II zones would be expected to benefit from an externally applied uniaxial stress, in terms of the misfit strain contribution to their energy barrier for nucleation, which would bias their nucleation on specific $\{111\}_{Al}$ habit plane variants aligned with the imposed stress field. The SAXS data further suggests that these plate shaped zones are preferentially aligned on $\{111\}_{Al}$, habit planes tilted at around ~ 35° to the tensile stress axis. Under stress-ageing conditions the GP-II zones appear to be more stable than the GP-I zones they replace and are smaller in size. They also have a higher Zn/Mg ratio, more similar to that seen in higher Zn/Mg ratio alloys and η′, and possibly a lower Cu content than GP-I zones. This change in dominance of the preferred zone in favor if GP-II zones appears to lead to a slightly higher rate of softening on early stage ageing at 108°C relative to the naturally aged condition, due to the greater change in volume fraction of the GP-I zones compared to in the stress-free sample.

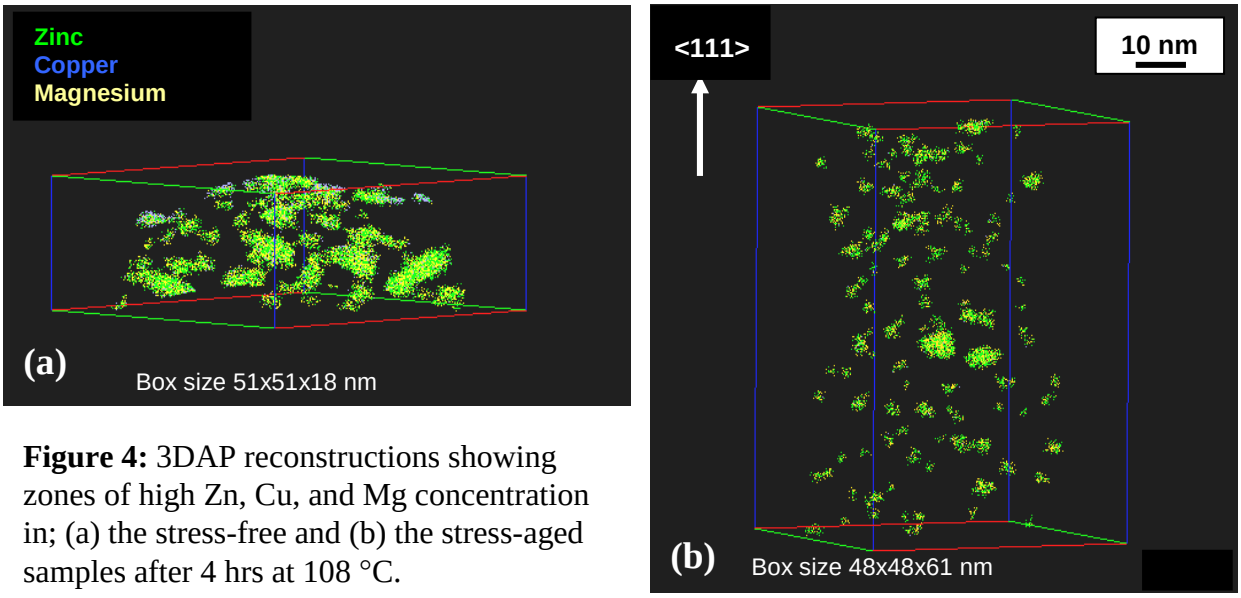

Figure 4: 3DAP reconstructions showing zones of high Zn, Cu, and Mg concentration in; (a) the stress-free and (b) the stress-aged samples after 4 hrs at 108 °C.

		Zn/Mg ratio	(Zn+Cu)/Mg ratio	Fraction (%)	Average size (atoms)	Aspect Ratio
Unloaded	High Zn/Mg	1.35±0.09	1.51±0.1	7	956	2.6
	Low Zn/Mg	1.02±0.06	1.17±0.05	93	172	1.2
Loaded	High Zn/Mg	1.34±0.11	1.38±0.14	72	37	1.75 (2.5)
	Low Zn/Mg	1.16±0.09	1.20±0.09	28	82	1.0

Table 1: Summary of 3DAP data for the 7475 alloy aged for 4 hrs at 108 °C, with and without an applied tensile stress, showing the average second phase composition, fraction, size, and aspect ratio, discriminated into two groups based on composition. Note the aspect ratio in brackets excludes data from very small clusters of less than 25 atoms.

3 Conclusions

Combined HRTEM, SAXS and 3DAP analysis has reveled that the application of a constant applied stress during early stage artificial ageing of a 7475 alloy can result in subtle, but significant, changes in precipitation behavior. The presence of a far-field tensile stress promotes thin plate shaped GP-II zones at the expense of GP-I zones, resulting in a lower net GP zone volume fraction and slight loss of strength. In the stress-aged samples smaller GP-II zones are observed preferentially oriented on $\{111\}_{Al}$ habit planes lying ~ 35° to the tensile stress axis. The GP-II zones have a higher Zn/Mg ratio and lower Cu content than GP-I zones in the stress-free sample.

Acknowledgements

This research was funded by the EPSRC through the Manchester LATEST Portfolio Partnership (EP/D029201/1 and the UK Atom probe analysis facility (Opal) (EP/077664/1). The authors are also grateful to Alcan for provision of materials and G. Grossman, and K. Geraki (CCLRC Daresbury) for assistance with the SAXS experiments.

4 References

[1] Skrotzki, B., Shiflet, G.J., Starke. E.A. Jr., Met. Mater. Trans., **1996,** *27A* , 3431-3444.
[2] Zhu, A.W., Starke, E.A. Jr., Acta Mater., **2001**, *49*, 2285-2295.
[3] Bakavos, D., Prangnell, P.B., Dif, R., Mat. Sci. Forum, **2004**, *28*, 124-131.
[4] Bakavos, D., Prangnell, P.B., Bes, B., Eberl, F., Gardiner, S., Mat. Sci. Forum, **2006**, *519-521*, 124-131.
[5] Hargarter, H., Lyttle, M.T., Starke, E.A., Mater. Sci. Eng., **1998**, *A257*, 87-99.
[6] Bakavos, D., Prangnell, P.B., Bes, B., Eberl, F., Mater. Sci. and Eng., 2008, doi:10.1016/j.msea.2008.03.014.
[7] Bakavos, D., Prangnell, P.B., Bes, B., Eberl, F., Grossman, G., Mat. Sci. Forum, **2006**, *519-521*, 333-338.
[8] Robey, R.F., Prangnell, P.B., Dif, R., Mater. Sci. Forum, **2004**, *28*, 132-138.
[9] Deschamps, A: *Analytical Techniques for aluminium alloys, Handbook of Aluminium*, Marcel Dekker Inc., New York, USA, **2003**, *2*, 155-170.
[10] Berg, L.K., Gjones, J., Hansen, V., Li, X.Z., Knutson-Wedel, M., Waterloo, G. Schryvers, D., and Wallenberg, L.R., Acta Mater., **2001**, *49*, 3343-3451.
[11] Stiller, K., Warren, P.J., Hansen, V., Angnete, J., Gjones, J., Mat. Sci. Eng.**1999,** *270*. 55-63.
[12] Kompatscer, M., Schonfeld, M., Heinric, B., Kostorz, H., J. Apl. Crystall. **2000**, *136*, 488-491.
[13] Chinh, N.Q., Ledvai, J., Ping, D.H., Hono, K., J. Alloys Compounds, **2004**, *378*, 52-60.
[14] Sha, G., Cerezo, A., Acta Mater., **2004**, *52*, 4503-4516.
[15] Engdahl, T., Hansen, V., Warren, P.J., Stiller, K., Mat. Sci. Eng., **2002**, *A327*, 59-64.
[16] Sha, G., Cerezo, A., Surf.Interface Anal., **2004**, *36*, 564-568.
[17] Ortner, S.R., Grovenor, C.R.M., and Shollock, B.A. Scripta Metall.,**1988**,*22*, 839-842.

[18] Bigot, A., Danoix, F., auger, P, Blavette, D., Reeves, A., Mat..Sci.Forum, **1996**, *217-222*, 695-700.